Structure, Vol. 10, 1551–1557, November, 2002, ©2002 Elsevier Science Ltd. All rights reserved. PII S0969-2126(02)00885-7

# NMR Structure of the Heme Chaperone CcmE Reveals a Novel Functional Motif

**Elisabeth Enggist,[1] Linda Thöny-Meyer,[1,4] Peter Güntert,[3] and Konstantin Pervushin[2,4]**
[1]Institut für Mikrobiologie
[2]Laboratorium für Physikalische Chemie
Eidgenössische Technische Hochschule
CH-8092 Zürich
Switzerland
[3]RIKEN Genomic Sciences Center
W505, 1-7-22 Suehiro
Tsurumi, Yokohama 230-0045
Japan

## Summary

**The concept of metal chaperones involves transient binding of metallic cofactors by specific proteins for delivery to enzymes in which they function. Metal chaperones thus provide a protective, as well as a transport, function. We report the first structure of a heme chaperone, CcmE, which comprises these two functions. We propose that the covalent attachment of heme to an exposed histidine occurs after heme binding at the surface of a rigid molecule with a flexible C-terminal domain. CcmE belongs to a family of proteins with a specific fold, which all share a function in delivery of specific molecular cargo.**

## Introduction

Heme is the redox-active cofactor of cytochromes involved in respiratory and photosynthetic electron transfer, the prosthetic group of numerous proteins, like hemoglobins, catalases, peroxidases, guanylate cyclase, and NO synthase [1], or the sensor of regulatory pathways for $O_2$-, CO-, or NO-dependent gene expression [2]. Transport and delivery of heme to the proteins that carry it are scarcely understood. We have discovered a bacterial heme chaperone, CcmE, which binds heme in the periplasm and delivers it to cytochromes of the *c* type [3]. It thus acts as an intermediate of a heme delivery pathway during cytochrome *c* biogenesis (Figure 1). CcmE is conserved in more than 25 organisms, including $\alpha$- and $\gamma$-proteobacteria, deinococci, and plant mitochondria. The alignment of seven representative sequences (Figure 2) shows a large number of highly conserved residues within the CcmE homologs. A hallmark of this protein is the covalent linkage between heme and histidine 130 of the polypeptide. This bond is formed transiently, and its chemical nature is not known. CcmE has a chaperone function, protecting the cell from premature activities of the highly reactive metalloorganic cofactor, which could cause oxidative damage. Additionally, CcmE is necessary for heme transfer, a function implying special dynamic properties of the polypeptide. The protein is anchored to the membrane with an N-terminal, hydrophobic domain (Figure 2). The hydrophilic, C-terminal domain is exposed to the periplasm, where attachment of heme to *c*-type cytochromes takes place [3]. The heme chaperone is a subunit of a cytochrome *c* maturation complex, in which it interacts directly with two multispanning membrane proteins, CcmC and CcmF. CcmC is required for the covalent binding of heme to CcmE [4, 5], whereas CcmF is involved in the detachment of heme from CcmE and its transfer to cytochrome *c* [6]. Therefore, we can predict a heme binding site and specific recognition sites for CcmC and CcmF to be present in the CcmE polypeptide. To understand the molecular mechanism of heme transfer to and from CcmE, which involves forming and breaking a covalent bond, we need the structures of both the hemeless apoform and the heme binding holoform of CcmE. Here, we present the NMR solution structure of the soluble part (residues L30–S159) of apo-CcmE from *E. coli*. It is the first structure of a protein involved in heme delivery during cytochrome *c* maturation. On the basis of this structure, we propose a model of holo-CcmE using (1) an analysis of positions of highly conserved residues in the protein structure, (2) effects of mutations of individual amino acids on heme binding and transfer properties, and (3) NMR spectra of the reduced holo-CcmE.

## Results and Discussion

### NMR Solution Structure of Apo-CcmE

The structure of the soluble domain of apo-CcmE shows two subdomains that are flexibly oriented relative to each other in solution (Figure 3A). The structure of the N-terminal subdomain (residues I34–H130) displays high atomic precision, with a root-mean-square deviation (rmsd) of 0.6 Å for backbone heavy atoms (Table 1), constituting a well-defined core of the protein. This domain is formed by a six-stranded $\beta$ sheet wrapped to a closed $\beta$ barrel capped by an $\alpha$ helix. The key residue H130 is strategically placed on the surface of the $\beta$ barrel near a solvent-exposed hydrophobic platform built by the conserved residues F37, V110, and L127 (Figure 3A). The structurally less-well-defined C-terminal subdomain contains a single helical turn (Figure 3B) followed by an unstructured tail of 16 residues (not shown in the structure). The conserved residues linking the two subdomains, H130–E132, and the three amino acids Y134, P136, and E138 face the same side of the subdomain (Figure 3B). The unstructured tail represents the least-conserved part of the protein with respect to both the length and amino acid composition (Figure 2).

The $^{15}N$ relaxation measurements indicate an isotropic rotational diffusion of apo-CcmE, with the rotational correlation time of 12 ns. The model-free analysis of the intramolecular dynamics confirms a rather restricted local conformational mobility of the amide moieties in the

[4]Correspondence: kopeko@phys.chem.ethz.ch (K.P.), lthoeny@micro.biol.ethz.ch (L.T.-M)

**Key words:** cytochrome *c* biogenesis; dynamic functional motif; heme chaperone; NMR

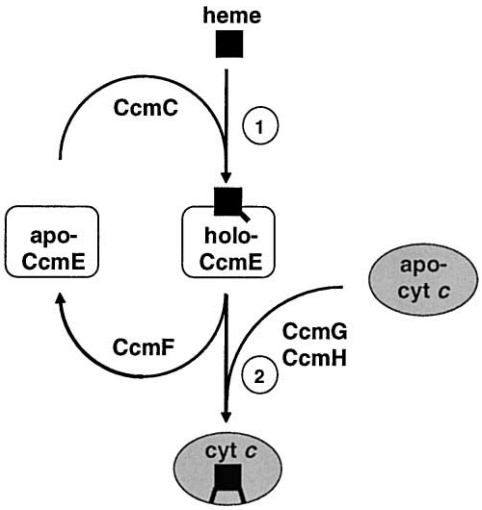


Figure 1. Role of the Heme Chaperone CcmE in Cytochrome *c* Maturation

Holo-CcmE contains covalently bound heme. Heme attachment to CcmE (1) requires CcmC; heme release and ligation to apocytochrome *c* (2) requires CcmF and the redox system CcmG/H.

core subdomain, with the average generalized order parameter of 0.82. The loop formed by residues R48–T50 exhibits slightly increased dynamical disorder on the nanosecond time scale as well as the conformational exchange $^{15}N$ line broadening in the millisecond timescale (Figure 3C). The average order parameter of 0.5 for the residues D131–M143 indicates, together with the well-defined local structure, mobility of the entire fragment relative to the core subdomain. The relative mobility of the two subdomains might be an intrinsic feature of the CcmE protein with respect to heme binding and delivery, enabling a dynamic access and release of the large heme group to and from the hydrophobic platform on the protein surface and the key residue H130, respectively, and protecting the highly reactive heme group once it is bound.

## Heme Binding of CcmE

Heme binding by apo-CcmE might first involve the formation of a noncovalent heme-CcmE complex. This binding could be stereospecific, depending on the shape of the heme binding pocket. Upon addition of hemin to apo-CcmE, a tight noncovalent complex was formed, which was detected by a heme-stainable band, even after SDS-polyacrylamide gel electrophoresis, but not by MALDI analysis. The absorption spectrum of the dithionite-reduced complex resembled that of a *b*-type cytochrome, with absorption maxima at 423, 530, and 559 nm, which were absent in control spectra of heme alone or heme plus bovine serum albumin (data not shown). In a second step the chemical reaction between the imidazole group of H130 and one of the vinyl groups of heme occurs, fixing heme in its position. In the covalent complex, holo-CcmE displays absorption maxima shifted to shorter wavelengths [3] (E. Enggist et al., submitted). However, it retains much of its secondary structure, as judged from the positions of the crosspeaks in TOCSY spectra of the reduced form of the protein, where interpretable NMR spectra can be obtained (data not shown).

Prior to this work, the precise location of the covalently or noncovalently bound heme within CcmE was not known. On the basis of the apo-CcmE structure, the positions of conserved residues, and site-directed mutagenesis of them (E. Enggist et al., submitted), we present a model for heme binding of CcmE, as shown in Figure 4. The heme binding H130 lies within the strictly conserved motif $^{126}$VLAKHDE$^{132}$, which is located at the interface between the core and the flexible subdomain. Heme can be docked to the surface of the CcmE core formed by the conserved hydrophobic residues F37, V110, and L127 and the basic residues R61 and K129. In our model the two basic residues are optimally positioned to interact with the propionate side chains of heme. The solvent-accessible side of heme can be shielded by the conserved I34 of the core subdomain and Y134 of the flexible subdomain to prevent redox reactions. Changes of F37, L127, or Y134 to alanine yielded mutants that were strongly affected in heme binding and subsequent transfer to cytochrome *c*. In the TOCSY spectra of reduced holo-CcmE, the side chain, but not the backbone, resonances of F37, R61, and V110, as well as many resonances of the flexible subdomain (residues 130–144), are significantly perturbed.

CcmE displays a distinct and novel heme binding motif, which thus far has not been described in other heme proteins. In hemoglobin, myoglobin, or *c*-type cytochromes, which contain heme as a permanently bound cofactor, the iron-protoporphyrin is buried inside a cavity. Likewise, in the heme biosynthesis and degradation enzymes ferrochelatase [7] and heme oxygenase [8], respectively, the tetrapyrrole is inside the protein. In heme transport and heme storage proteins, heme is more exposed to the surface. The extracellular hemophore HasA captures heme by two long exposed loops. Binding occurs with high affinity without changing the conformation of the protein [9, 10]. In bacterioferritin, heme is placed in a hydrophobic pocket perpendicular to the surface, with the propionates directed inward into the solvent-filled cavity of the protein [11]. Hemopexin, the heme storage protein with the strongest affinity for its substrate, binds heme in a loop between two β propeller domains. The conformation of this loop is determined by the way it wraps around the heme [12]. Thus, the transient heme binding of CcmE is mediated by a novel functional motif featuring important intramolecular dynamic properties.

## A New Functional Motif

The DALI structural homology search [13] throughout the pool of known protein structures revealed a close 3D similarity between apo-CcmE and a number of proteins commonly classified to the so-called OB (oligonucleotide/oligosaccharide binding) fold [14, 15]. Among the structurally most-similar proteins are the chain C of the 32 kDa subunit of the replication protein A (*Homo sapiens*; DALI score, 9.4; rmsd, 2.8 Å) and the N-terminal domain of the aspartyl tRNA synthetase (*E. coli*; DALI

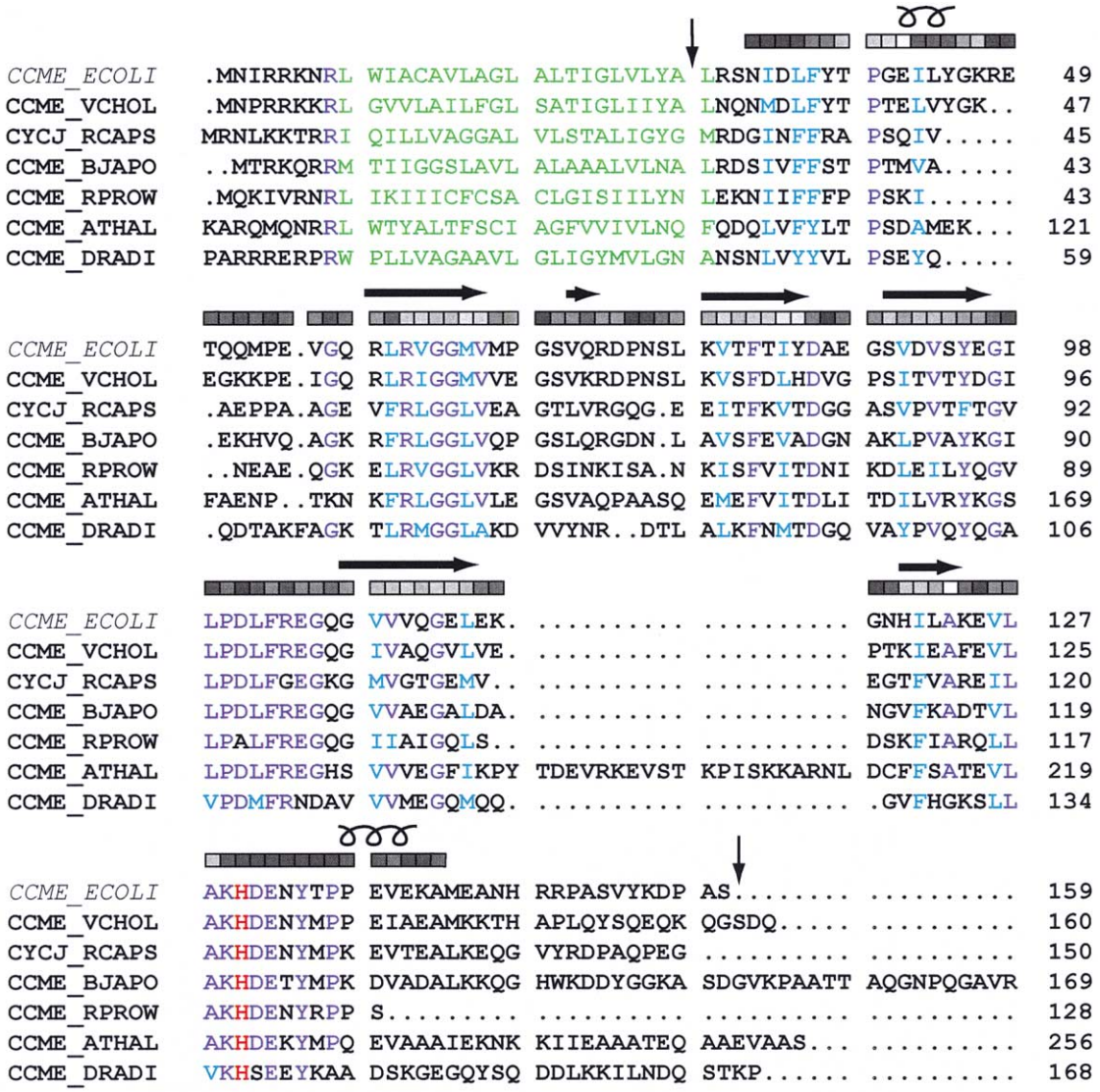


Figure 2. Alignment, Secondary Structure Elements, and Surface Exposure of CcmE

Dark blue, conserved residues (85%–100%); light blue, hydrophobic residues; green, membrane anchor; red, heme binding histidine. Secondary structure elements of *E. coli* CcmE are shown on the top. Shaded rectangles denote the surface accessibility of the corresponding residues calculated with the program MOLMOL [27] (dark, exposed; bright, buried). The vertical arrows indicate the start and the end of the soluble construct from *E. Coli*. Sequence alignment was generated with T-Coffee [28] (http://www.ch.embnet.org/software/TCoffee.html). ECOLI, *Escherichia coli*; VCHOL, *Vibrio cholerae*; RCAPS, *Rhodobacter capsulatus*; BJAPO, *Bradyrhizobium japonicum*; RPROW, *Rickettsia prowazekii*; ATHAL, *Arabidopsis thaliana*; DRADI, *Deinococcus radiodurans*.

score, 8.8; rmsd, 2.4 Å). Figure 5 shows the 3D similarity between apo-CcmE and these proteins, including the topology and the geometry of the β barrel, the length of loops, and the positions of domain linkers. In all cases the compact β barrel core is linked to an α helix, which mediates interactions with another polypeptide or domain. In the replication protein A, this helix is involved in complex formation between chains C and D [16]. In the aspartyl tRNA synthetase, it interacts with the C-terminal domain [17]. Despite the structural similarity these proteins feature neither sequence homologies nor share the same function. Nevertheless, they all transiently bind nonprotein molecules, activate them, and deliver them selectively to an acceptor protein. However, specific binding of their cargo molecule at the surface of the rigid core occurs at different positions. With CcmE as a new member of proteins sharing this fold, we propose a new functional motif consisting of the β barrel core subdomain flexibly linked to the α helical domain, ensuring essential conformational mobility to grant the access of ligands to the binding site and to protect them from the solvent by the subsequent delivery to a specific acceptor protein. Since this new motif is not restricted to the binding of oligonucleotides and oligosaccharides, as indicated by the name "OB fold," we suggest that it be called, more generally, a cargo motif. In CcmE, this motif is suitable for transiently accomodating heme but also allows specific interactions with the heme donor

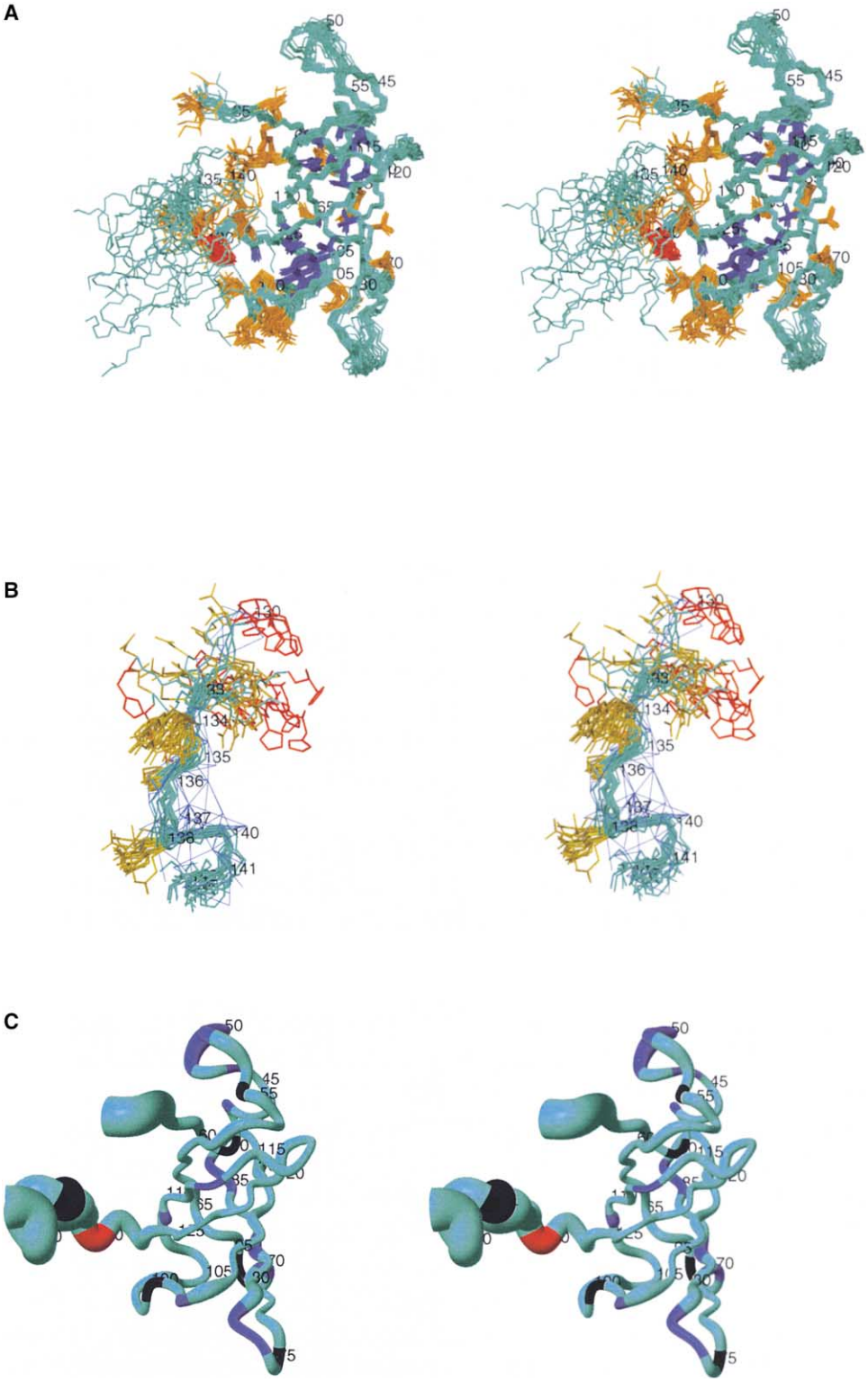


Figure 3. NMR Solution Structure and Intramolecular Dynamics of Apo-CcmE

Overlay in stereo of the backbone of the 20 NMR structural conformers, (A) residues 34–143 superimposed with residues 37–130 and (B) residues 130–143 superimposed with residues 133–141. The side chains of the highly conserved and solvent-accessible or buried residues are shown in orange and blue, respectively. In (B), blue lines show the network of NOE-derived proton-proton distance constraints for one conformer.

(C) A stereo spline representation of a conformer with the variable radius of the tube set to $4 \times (1 - S^2)$, where $S^2$ is the generalized order parameter of the local angular dynamics of the HN vectors. Residues in dark blue exhibit more than 1 $s^{-1}$ conformational exchange-induced transverse $^{15}N$ relaxation. The residues are in black when the dynamical information is not available (e.g., for prolines). The heme binding residue H130 is shown in red.

Table 1. Structural Statistics for CcmE

| Quantity | Value[a] |
|---|---|
| NOE upper distance limits (long range, medium range) | 2453 (970, 936) |
| Dihedral angle constraints | 56 |
| DYANA target function value (Å$^2$) | 1.97 ± 0.56 |
| Distance constraint violations | |
| Number greater than 0.2 Å | 0 |
| Maximum (Å) | 0.14 ± 0.01 |
| Dihedral angle constraint violations | |
| Number greater than 5° | 0 |
| Maximum (°) | 1.5 ± 0.7 |
| AMBER energies (kcal/mol) | |
| Total | −4238 ± 101 |
| van der Waals | −278 ± 18 |
| Electrostatic | −4959 ± 93 |
| Rms deviation from ideal geometry: | |
| Bond lengths (Å) | 0.0079 ± 0.0002 |
| Bond angles (°) | 2.12 ± 0.06 |
| Rms deviation to the averaged coordinates (Å) | |
| N, Cα, C′ (35–130) | 0.59 ± 0.09 |
| All heavy atoms (35–130) | 1.07 ± 0.14 |
| Rms deviations from experimental data | |
| Average distance constraint violation (Å) | 0.0178 ± 0.0005 |
| Average dihedral angle constraint violation (°) | 0.25 ± 0.09 |
| Ramachandran analysis | |
| Residues in favored regions | 66% |
| Residues in additionally allowed regions | 28% |
| Residues in generously allowed regions | 4% |
| Residues in disallowed regions | 2% |

[a] Except in the top two entries, the average for the 20 energy-minimized conformers with the lowest residual DYANA target function values and the standard deviation among them are given.

CcmC and the heme acceptor CcmF, which both were shown to coprecipitate with CcmE [5, 6]. These interactions may require conformational changes within CcmE, which are possible because of the highly dynamic features provided by the cargo motif.

## Biological Implications

The structure of the heme chaperone CcmE represents the first example of an intracellular heme delivery device. Unlike other heme proteins, CcmE displays a rigid core with a hydrophobic surface that is suitable for heme binding, in agreement with our observation of noncovalent heme binding to CcmE in vitro. A key function appears to be the flexible α-helical domain of the protein, which is strategically positioned in the vicinity of the heme binding site. This domain can protect transiently bound heme from interactions with other molecules, and, because of its flexibility, can aid in the delivery of heme. On the basis of the reported high-resolution 3D structure of apo-CcmE, the model of the heme-CcmE complex, and functional biochemical studies of the Ccm system (Enggist et al., submitted), we propose a general mechanism of the heme delivery. First, the heme group is transferred across the cytoplasmic membrane of *E. coli* to a membrane-bound form of apo-CcmE, where it binds to a hydrophobic interface at the surface of the β barrel core of CcmE. The membrane protein CcmC is required for this transfer (Figure 1). A covalent bond to H130 is then formed, and the flexible C-terminal domain is bent to shield heme. Upon interaction with the downstream protein CcmF, heme is released and transferred

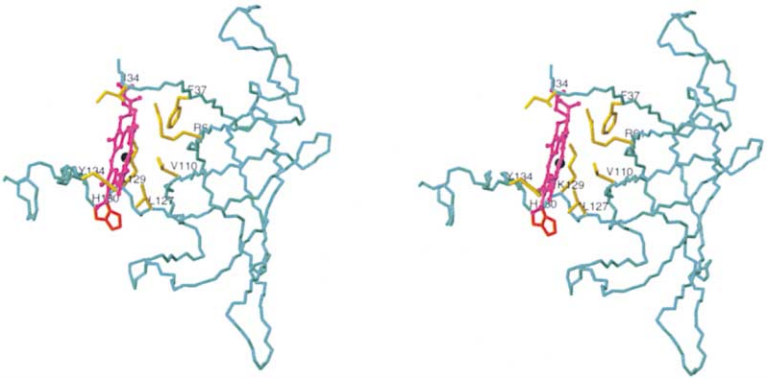


Figure 4. Model of the CcmE Structure in a Covalent Complex with Heme

The heme group shown in magenta with the Fe ion in black is covalently bound via the vinyl 2 group to the $N^{\delta 1}$ atom of the imidazole ring of H130 (red). The side chains of the solvent-exposed and conserved residues I34, F37, R61, V110, L127, K129, and Y134, which form a putative heme binding site on the protein surface, are shown in yellow. R61 was slightly rotated toward the propionate group of heme. Both N- and C-terminal subdomains may adjust their conformation in holo-CcmE to protect the hydrophobic heme from the solvent.

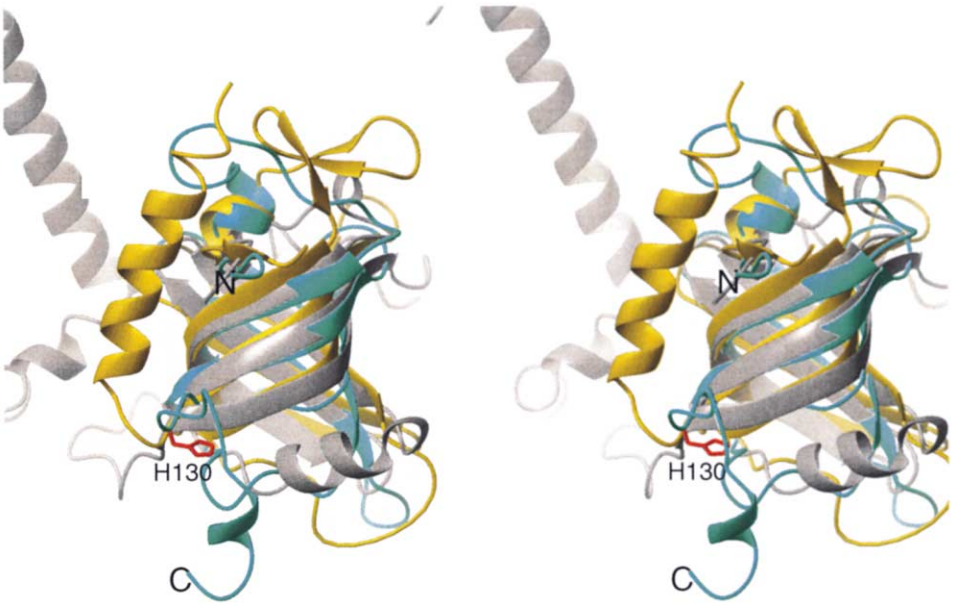


Figure 5. Overlay, in Stereo, of the Backbone of the Apo-CcmE Conformer with Two Structurally Similar Proteins

Apo-CcmE is shown in blue. Chain C of the 32 kDa subunit of the human replication protein (Protein Data Bank code 1quq), shown in yellow, and the N-terminal domain of aspartyl tRNA synthetase (Protein Data Bank code 1c0a), shown in gray, were found by the DALI search [29]. Protein Data Bank residue numbers of aligned segments are as follows (CcmE/1quq-A): 36–46/47–57, 47–52/66–71, 58–68/72–82, 71–74/83–86, 77–89/87–99, 90–97/101–108, 101–117/118–134, 118–132/138–152. In the second superposition Protein Data Bank residue numbers of aligned segments are as follows (CcmE/1c0a): 37–44/3–10, 54–68/12–26, 71–76/27–32, 79–95/33–49, 96–99/57–60, 101–117/61–77, 118–132/91–105. The side chain of H130 in CcmE is shown in red.

to cytochrome *c* [6], most likely also involving a movement of the flexible domain. The molecular dynamical properties of the CcmE protein, which accommodates both heme chaperone and transfer functions, originate from a specific fold. It groups CcmE together with the OB fold family of proteins, extending their family to the cargo fold proteins, with the typical characteristic of having helical domains linked to a β barrel core. These proteins exert functions that involve transient binding and specific delivery of substrate molecules.

## Experimental Procedures

### Protein Purification and NMR Samples

Apo-CcmE-$H_6$ (residues 30–159) was expressed and purified as described in E. Enggist et al. (submitted). The presence of the $His_6$-tag ($H_6$) at the C terminus does not interfere with the function of the protein. The Δ*ccmA-H* strain EC06 was transformed with pEC415, encoding soluble CcmE-$H_6$ [3], and grown in 1 liter of Celtone-CN (Martek) supplemented with 100 μg/ml ampicillin. At $OD_{600}$ = 1.0, cells were induced with 0.05% arabinose. After extraction of the periplasmic proteins, ammonium sulfate precipitation, and affinity chromatography, the sample was dialyzed against 300 mM NaCl and 50 mM sodium phosphate (pH 7.2) and concentrated to 1.1 mM. Soluble holo-CcmE-$H_6$ was isolated from 20 liters of LB medium and separated from apo-CcmE-$H_6$ by hydrophobic interaction chromatography as described elsewhere (Enggist et al., submitted). The final concentration was 1.2 mM.

### Visible Absorption Spectroscopy

Optical spectra were recorded on a Hitachi model U-3300 spectrophotometer. If necessary, samples were reduced by adding a few grains of sodium dithionite. A 1 mM hemin solution at pH 7.2 was added to a 100 μM solution of nonlabeled apo-CcmE. Spectra were recorded immediately after mixing.

### NMR Spectroscopy

NMR experiments were performed at 30°C on five-channel Bruker Avance 600 and 800 NMR spectrometers equipped with pulsed-field gradients. NMR experiments included 2D [$^{15}$N,$^{1}$H]-TROSY, 3D TROSY-HNCA and -HNCACB [18], and conventional CBCA(CO)NH, HCCH-TOCSY, $^{15}$N-edited TOCSY, $^{15}$N-edited NOESY ($\tau$ = 60 ms), $^{13}$C-edited NOESY ($\tau$ = 60 ms), $^{13}C^{aromatic}$-edited NOESY ($\tau$ = 60 ms), 2D NOESY ($\tau$ = 60 ms), and 2D TOCSY [19]. The intramolecular dynamics were studied by $^{15}$N $T_1$, $T_{1\rho}$, and {$^{1}$H}-$^{15}$N heteronuclear NOE relaxation measurements [20] and interpreted with the isotropic model-free approach in DASHA [21].

### NMR Structure Calculations

Constraints for 28 $\phi$ and 28 $\psi$ backbone torsion angles were derived from Cα secondary chemical shifts (Table 1). A total of 6335 NOESY crosspeaks were picked in the aforementioned three NOESY spectra with the program XEASY [22] and assigned with the automated NOESY crosspeak assignment method CANDID [23] in the program DYANA [24]. Seven cycles of automated NOESY assignment with CANDID and then structure calculation with the torsion angle dynamics algorithm of DYANA [24] were performed. In all cycles, structure calculations were started from 100 random conformers, and the standard simulated-annealing schedule of DYANA was used with 16,000 torsion angle dynamics steps per conformer. In the final CANDID cycle, 6220 NOESY crosspeaks (98%) were assigned unambiguously, of which 1720 connected protons separated by more than five residues in the protein sequence, leading to 2453 meaningful NOE distance constraints. The 20 conformers with the lowest target function values after the seventh CANDID/DYANA cycle were further energy minimized in a water shell with respect to the AMBER force field [25] with the program OPALp [26] (Table 1). The resulting bundle of 20 energy-refined DYANA conformers represents the solution structure of CcmE. The program MOLMOL [27] was used for the analysis of the structure and for the preparation of figures.

**Acknowledgments**

We thank Tim Heinz for his help in $^{15}N$ relaxation data analysis. This work was supported by grants from the Swiss National Foundation for Scientific Research to L.T.-M.

Received: May 29, 2002
Revised: July 30, 2002
Accepted: August 1, 2002

**References**

1. Ponka, P. (1999). Cell biology of heme. Am. J. Med. Sci. *318*, 241–256.
2. Rodgers, K.R. (1999). Heme-based sensors in biological systems. Curr. Opin. Chem. Biol. *3*, 158–167.
3. Schulz, H., Hennecke, H., and Thöny-Meyer, L. (1998). Prototype of a heme chaperone essential for cytochrome *c* maturation. Science *281*, 1197–1200.
4. Schulz, H., Fabianek, R.A., Pellicioli, E.C., Hennecke, H., and Thöny-Meyer, L. (1999). Heme transfer to the heme chaperone CcmE during cytochrome *c* maturation requires the CcmC protein, which may function independently of the ABC-transporter CcmAB. Proc. Natl. Acad. Sci. USA *96*, 6462–6467.
5. Ren, Q., and Thöny-Meyer, L. (2001). Physical interaction of CcmC with heme and the heme chaperone CcmE during cytochrome *c* maturation. J. Biol. Chem. *276*, 32591–32596.
6. Ren, Q., Ahuja, U., and Thöny-Meyer, L. (2002). A bacterial cytochrome *c* heme lyase. CcmF forms a complex with the heme chaperone CcmE and CcmH but not with apocytochrome *c*. J. Biol. Chem. *277*, 7657–7663.
7. Al-Karadaghi, S., Hansson, M., Nikonov, S., Jonsson, B., and Hederstedt, L. (1997). Crystal structure of ferrochelatase: the terminal enzyme in heme biosynthesis. Structure *5*, 1501–1510.
8. Schuller, D.J., Wilks, A., Ortiz de Montellano, P.R., and Poulos, T.L. (1999). Crystal structure of human heme oxygenase-1. Nat. Struct. Biol. *6*, 860–867.
9. Arnoux, P., Haser, R., Izadi, N., Lecroisey, A., Delepierre, M., Wandersman, C., and Czjzek, M. (1999). The crystal structure of HasA, a hemophore secreted by *Serratia marcescens*. Nat. Struct. Biol. *6*, 516–520.
10. Létoffé, S., Nato, F., Goldberg, M.E., and Wandersman, C. (1999). Interactions of HasA, a bacterial haemophore, with haemoglobin and with its outer membrane receptor HasR. Mol. Microbiol. *33*, 546–555.
11. Cobessi, D., Huang, L.S., Ban, M., Pon, N.G., Daldal, F., and Berry, E.A. (2002). The 2.6 Å resolution structure of *Rhodobacter capsulatus* bacterioferritin with metal-free dinuclear site and heme iron in a crystallographic 'special position'. Acta Crystallogr. D Biol. Crystallogr. *58*, 29–38.
12. Paoli, M., Anderson, B.F., Baker, H.M., Morgan, W.T., Smith, A., and Baker, E.N. (1999). Crystal structure of hemopexin reveals a novel high-affinity heme site formed between two beta-propeller domains. Nat. Struct. Biol. *6*, 926–931.
13. Holm, L., and Sander, C. (1996). Mapping the protein universe. Science *273*, 595–603.
14. Murzin, A.G. (1993). OB(oligonucleotide/oligosaccharide binding)-fold: common structural and functional solution for non-homologous sequences. EMBO J. *12*, 861–867.
15. Mitton-Fry, R.M., Anderson, E.M., Hughes, T.R., Lundblad, V., and Wuttke, D.S. (2002). Conserved structure for single-stranded telomeric DNA recognition. Science *296*, 145–147.
16. Bochkarev, A., Bochkareva, E., Frappier, L., and Edwards, A.M. (1999). The crystal structure of the complex of replication protein A subunits RPA32 and RPA14 reveals a mechanism for single-stranded DNA binding. EMBO J. *18*, 4498–4504.
17. Eiler, S., Dock-Bregeon, A., Moulinier, L., Thierry, J.C., and Moras, D. (1999). Synthesis of aspartyl-tRNA(Asp) in *Escherichia coli*—a snapshot of the second step. EMBO J. *18*, 6532–6541.
18. Salzmann, M., Wider, G., Pervushin, K., Senn, H., and Wüthrich, K. (1999). TROSY-type triple-resonance experiments for sequential NMR assignments of large proteins. J. Am. Chem. Soc. *121*, 844–848.
19. Cavanagh, J., Fairbrother, W.J., Palmer, A.G., and Skelton, N.J. (1996). Protein NMR Spectroscopy: Principles and Practice (New York: Academic Press).
20. Luginbühl, P., Pervushin, K.V., Iwai, H., and Wüthrich, K. (1997). Anisotropic molecular rotational diffusion in $^{15}N$ spin relaxation studies of protein mobility. Biochemistry *36*, 7305–7312.
21. Orekhov, V.Y., Nolde, D.E., Golovanov, A.P., Korzhnev, D.M., and Arseniev, A.S. (1995). Processing of heteronuclear NMR relaxation data with the new software DASHA. Appl. Magn. Reson. *9*, 581–588.
22. Güntert, P., Dötsch, V., Wider, G., and Wüthrich, K. (1992). Processing of multi-dimensional NMR data with the new software PROSA. J. Biomol. NMR *2*, 619–629.
23. Herrmann, T., Güntert, P., and Wüthrich, K. (2002). Protein NMR structure determination with automated NOE assignment using the new software CANDID and the torsion angle dynamics algorithm DYANA. J. Mol. Biol. *319*, 209–227.
24. Güntert, P., Mumenthaler, C., and Wüthrich, K. (1997). Torsion angle dynamics for NMR structure calculation with the new program DYANA. J. Mol. Biol. *273*, 283–298.
25. Cornell, W.D., Cieplak, P., Bayly, C.I., Gould, I.R., Merz, K.M., Ferguson, D.M., Spellmeyer, D.C., Fox, T., Caldwell, J.W., and Kollman, P.A. (1995). A 2nd generation force-field for the simulation of proteins, nucleic-acids, and organic-molecules. J. Am. Chem. Soc. *117*, 5179–5197.
26. Koradi, R., Billeter, M., and Güntert, P. (2000). Point-centered domain decomposition for parallel molecular dynamics simulation. Comput. Phys. Commun. *124*, 139–147.
27. Koradi, R., Billeter, M., and Wüthrich, K. (1996). MOLMOL: a program for display and analysis of macromolecular structures. J. Mol. Graph. *14*, 51–55.
28. Notredame, C., Higgins, D.G., and Heringa, J. (2000). T-Coffee: a novel method for fast and accurate multiple sequence alignment. J. Mol. Biol. *302*, 205–217.
29. Holm, L., and Sander, C. (1993). Protein structure comparison by alignment of distance matrices. J. Mol. Biol. *233*, 123–138.

**Accession Numbers**

Coordinates have been deposited in the Protein Data Bank under accession code 1LIZ. $^{1}H$, $^{15}N$, and $^{13}C$ resonance assignments have been reported and deposited in the BioMagResBank under accession code BMRB-5526.

**Note Added in Proof**

The data referred to throughout as "Enggist et al., submitted" are now in press: Enggist, E., Schneider, M.J., Schulz, H., and Thöny-Meyer, L. (2002). Biochemical and mutational characterization of the heme chaperone CcmE reveals a heme binding site. J. Bacteriol., in press.